High temperature characteristics of a 2 µm InGaSb/AlGaAsSb passively mode-locked quantum well laser

Xiang Li, Hong Wang, Zhongliang Qiao, Xin Guo, Wanjun Wang, Jia Xu Brian Sia, Geok Ing Ng, Yu Zhang, Zhichuan Niu 🆔, Cunzhu Tong, and Chongyang Liu

View Online Export Citation CrossMark

ARTICLES YOU MAY BE INTERESTED IN

Growth and fabrication of GaN/Er:GaN/GaN core-cladding planar waveguides
Applied Physics Letters **114**, 222105 (2019); https://doi.org/10.1063/1.5093942

Iontronic control of GaInAsP photonic crystal nanolaser
Applied Physics Letters **114**, 221105 (2019); https://doi.org/10.1063/1.5098119

Optically tailored trapping geometries for ultracold atoms on a type-II superconducting chip
Applied Physics Letters **114**, 222601 (2019); https://doi.org/10.1063/1.5096997

Applied Physics Letters

Mid-IR and THz frequency combs
special collection

Read Now!

High temperature characteristics of a 2 μm InGaSb/AlGaAsSb passively mode-locked quantum well laser

Xiang Li,[1] Hong Wang,[1,a)] Zhongliang Qiao,[1,a)] Xin Guo,[1] Wanjun Wang,[1] Jia Xu Brian Sia,[1] Geok Ing Ng,[1] Yu Zhang,[3] Zhichuan Niu,[3,a)] (iD) Cunzhu Tong,[4] and Chongyang Liu[2]

AFFILIATIONS

[1]School of Electrical and Electronic Engineering, Nanyang Technological University, 50 Nanyang Avenue, 639798 Singapore
[2]Temasek Laboratories, Nanyang Technological University, 50 Nanyang Drive, 637553 Singapore
[3]State Key Lab for Superlattices and Microstructures, Institute of Semiconductors, Chinese Academy of Sciences, No.A35 QingHua East Road, Beijing 100083, China
[4]State Key Lab of Luminescence and Applications, Changchun Institute of Optics, Fine Mechanics and Physics, Chinese Academy of Sciences, No.3888 Dong Nanhu Road, Changchun 130033, China

[a)]Electronic addresses: ewanghong@ntu.edu.sg; zlqiao@ntu.edu.sg; and zcniu@semi.ac.cn

ABSTRACT

A monolithic two-section InGaSb/AlGaAsSb single quantum well mode-locked laser (MLL) emitting at 2 μm is demonstrated. The laser is able to lase in the continuous wave mode up to 80 °C, and passive mode locking operation with a fundamental repetition frequency of $\sim$18.4 GHz is observed up to 60 °C. The laser has a characteristic temperature T_0 of $\sim$88 K near room temperature, which is only slightly affected by the absorber bias voltage (V_a). One consequence of this finding is verified by the temperature-independent power ratios before lasing. The variations of the repetition frequency with gain current (I_g) and temperature (T) have also been systematically investigated. In the bias range in this work, the repetition frequency increases as a whole by more than 30 MHz when the temperature is raised from 20 to 40 °C. Frequency tuning of $\sim$130 and $\sim$60 MHz was observed at 20 and 40 °C, respectively. The results and their mechanism analysis provide guidelines for GaSb-based MLLs to better meet the application-required repetition frequencies even with the presence of an unwanted increase in temperature.

Published under license by AIP Publishing. https://doi.org/10.1063/1.5096447

High-frequency optical pulse trains are desirable for a number of applications in chemistry, sensing, communication, and military.[1–3] By virtue of its capability in generating such pulse trains, mode-locked semiconductor lasers attract great attention by taking advantage of their flexible wavelength tuning, compactness, high efficiency, and easy electrical pump, as well as integration opportunities with silicon photonics.[4,5] In addition, their two-/multisection configurations enable us to greatly simplify the setup and obtain totally monolithic devices.

Stable mode locking has been demonstrated in a variety of monolithic two-/multisection semiconductor lasers at several wavelengths, e.g., 400 nm GaN-based quantum well (QW) lasers,[6] 1.3 μm GaAs-based quantum dot (QD) lasers,[7–9] 1.5 μm InP-based quantum well,[10] quantum dot,[11,12] and quantum dash lasers.[13,14] More recently, Merghem *et al.* and our group also reported passive mode locking of GaSb-based quantum well lasers in the 2 μm wavelength range,[15,16] and Feng *et al.* further extended the wavelength to 3.25 μm with a GaSb-based cascade laser.[17] These longer wavelengths are very useful

for molecular spectroscopy, gas sensing, free-space, and advanced telecommunications and eye-safe light detection and ranging (LIDAR).[18–20] Despite these numerous achievements, high temperature characteristics of these lasers, especially GaSb-based ones, are rarely studied. To be specific, the characteristic temperature T_0 as well as the effects of the absorber bias voltage on it and high temperature mode locking characteristics (e.g., repetition frequency, spectrum, and so on) remain unclear. These issues are important when the mode-locked lasers (MLLs) are used as light sources at high temperatures, which is inevitable in many applications.

In this work, stable mode locking up to 60 °C is demonstrated in a two-section InGaSb/AlGaAsSb single quantum well (SQW) laser emitting at 2 μm. Its characteristic temperature T_0 is investigated at different absorber bias voltages. The effects of working temperature (T) and injection current into the gain section (I_g) on the repetition frequency are experimentally obtained. The mechanisms behind the frequency variation are analyzed.

The epi-wafer used for device fabrication was grown on a (100) n-GaSb substrate by molecular beam epitaxy (MBE). The cladding layers are 2 μm-thick lattice-matched $Al_{0.5}GaAsSb$, while the undoped separate confinement heterostructure (SCH) layers are 270 nm-thick lattice-matched $Al_{0.25}GaAsSb$. The $In_{0.2}Ga_{0.8}Sb$ SQW is 10 nm-wide with a compressive strain of 1.26%.

Figure 1(a) shows an optical microscopy photograph of one cleaved laser bar which contains several two-section lasers, and an enlarged view of the region within the white frame is shown in Fig. 1(b). For the fabrication process, first, standard photolithography and wet chemical etching at room temperature were carried out to form the ridge. A SiO_2 layer was deposited on top of the wafer, and the contact window was opened by lithography and the following buffered oxide etch (BOE) process. After another step of photolithography to define the gain and absorber sections, as well as the electrical isolation region between them, Ti/Au was evaporated on top of the GaSb laser to form the p-side contact. Subsequent lift-off and wet etching processes realized the 10 μm-wide electrical isolation. In our fabrication, the high-conductivity contact layer and part of the p-cladding layer were etched off. A resistance of ~1.1 kΩ was achieved between the two sections with an etch depth of ~1.5 μm. In the end, the wafer was thinned to a thickness of ~120 μm, and Ni/Ge/Au/Ni/Au was evaporated to form the n-side contact. For the tested laser in this study, the ridge width is ~5 μm, which provides single lateral mode operation. The lengths of the gain section (L_g) and the absorber section (L_a) are 1.89 mm and 0.23 mm, respectively. The laser facets are as-cleaved without any coating. When working in the mode locking regime, the gain section is forward biased (I_g), while the absorber section needs to be reverse biased (V_a). A temperature electronic controller (TEC) was used for temperature control during the measurements.

The two-section laser under test lased in the continuous wave (cw) mode up to 80 °C. Figures 2(a) and 2(b) show the light output power collected from the facet of the gain section as a function of the injection current (L-I) for the tested laser at 20 and 80 °C. At 20 °C, V_a was varied from 0 to −3 V. The threshold current increases consistently with increasing negative V_a owing to the stronger absorption. At 80 °C, the laser was able to lase only when the absorber section is forward biased.

Stable mode locking was achieved in a wide range of bias conditions up to 60 °C. Figures 2(c) and 2(d) show a typical RF spectrum and the corresponding optical spectrum at 20 °C ($I_g = 120$ mA; $V_a = −1.2$ V). The RF spectrum was measured using a high-speed photo detector (EOT ET-5000F) followed by a 50 GHz RF spectrum
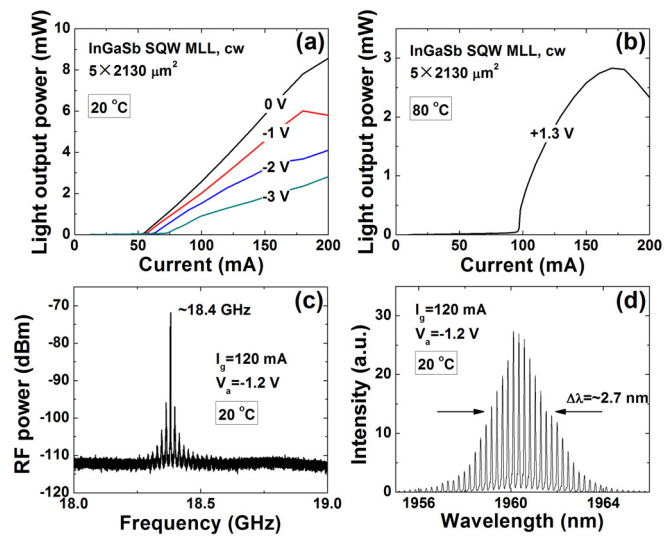
FIG. 2. L-I curves of the laser at (a) 20 °C (V_a varies from 0 to −3 V) and (b) 80 °C ($V_a = +1.3$ V). (c) and (d) show a typical RF spectrum and the corresponding optical spectrum at 20 °C ($I_g = 120$ mA; $V_a = −1.2$ V).

analyzer (Agilent N9030A). The fundamental repetition frequency at ~18.4 GHz is determined by the photon round-trip time in the 2.13 mm-long laser cavity. The optical spectrum has a full width at half maximum (FWHM) of ~2.7 nm, and more than 30 longitudinal modes spaced by ~0.237 nm are included. If unchirped sech2 function pulses are assumed which have a time-bandwidth product of ~0.315, a minimum pulse width of ~1.5 ps is expected. Using the pulse width estimation method in Ref. 15 gives a similar result.

The variation of the threshold current density J_{th} with temperature T for a semiconductor laser can be empirically expressed as

$$J_{th}(T) = J_0 \exp\left(\frac{T}{T_0}\right), \qquad (1)$$

where J_0 is a constant and T_0 is the characteristic temperature whose value is a measure of the temperature sensitivity of the threshold current density. To extract T_0, temperature dependences of J_{th} (on a logarithmic scale) when the absorber was biased at 0, −1, −2, and −3 V are obtained and shown in Fig. 3. On one hand, the threshold current densities increase with increasing negative V_a as expected. From the trend of these lines on the other hand, there is no obvious difference in T_0 between different V_a. T_0 is determined to be ~88 K near room temperature and decreases consistently when temperature rises. This T_0 is comparable to that of single-section GaSb-based quantum well lasers, whose typical T_0 is 60–80 K.[21,22] According to these results, at a certain fixed temperature, larger current is needed to compensate the additional loss introduced by the absorber when V_a is varied to a more negative value (0 to −1 V, −1 to −2 V, and −2 to −3 V). However, this additional loss has a negligible influence on the gain section's band structure and crystal quality, which dominate the temperature-dependent thermionic carrier emission, and thus has only slight effects on T_0. Similar results that T_0 is V_a-independent have also been reported in studies of an InP-based QW laser[23] and a GaAs-based QD laser.[9]
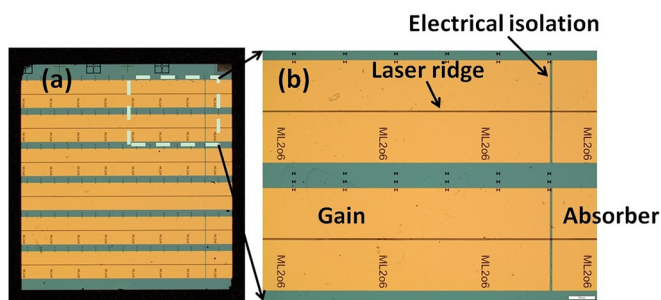

FIG. 1. (a) Optical microscopy photograph of one cleaved laser bar which contains several two-section lasers. (b) Enlarged view of the contents within the white frame in (a).
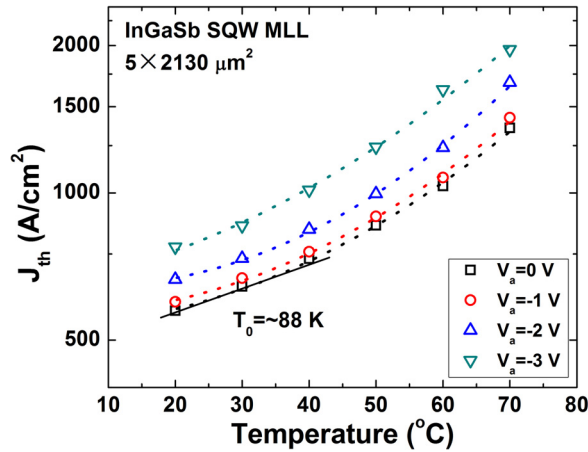
FIG. 3. Temperature dependences of the threshold current density (J_{th}, on a logarithmic scale) when the absorber was biased at 0, -1, -2, and -3 V.

FIG. 4. Ratios of the output powers at adjacent V_a from 20 to 70 °C at $I_g = 40$ mA.

If the coefficient of this additional loss is indicated as α_n, where n = 1 (0 to -1 V), 2 (-1 to -2 V), and 3 (-2 to -3 V), the intracavity intensity I_0 would drop to $I_0 \exp(-\alpha_n L_a)$ under the impact of the loss. Since both α_n and L_a are constants (when I_0 is weak), the ratios of the intensities at adjacent V_a (I_{0V}/I_{-1V}, I_{-1V}/I_{-2V}, I_{-2V}/I_{-3V}) should also be constants no matter what the temperature is. These ratios only reflect the certain losses introduced by the absorber when V_a is varied. Note that this conclusion is only applicable before lasing threshold since the absorber here is the so-called saturable absorber, which means that α_n introduced by it is intensity-dependent. Before lasing, the intracavity intensity is quite weak, and α_n will remain high and not change much with the intensity. In contrast, after lasing, there will be a rapid increase in the intracavity intensity, and α_n may change dramatically as a result. In addition, different working regimes emerge under some certain bias conditions after lasing. It changes from one bias condition to another, and α_n may also be different among these conditions.

To add more evidence on the above conclusion, the output power ratios at adjacent V_a from 20 to 70 °C at $I_g = 40$ mA (prelasing), which directly reflect the intracavity intensity ratios, were calculated and are shown in Fig. 4. As can be seen from the figure, all the three ratios only swing around specific values, and the maximum deviation from their mean values is only ~1%, which confirms the conclusion. The mean value of P_{-2V}/P_{-3V} is larger, which indicates that a larger loss is introduced when V_a is varied from -2 to -3 V.

As we know, the fundamental repetition frequency of a mode-locked laser, determined by the photon round-trip time in the 2.13 mm-long laser cavity, is expressed as

$$f = \frac{c}{2 n_{eff} L},$$ (2)

where c is the speed of light, n_{eff} is the effective refractive index, and L is the laser cavity length. In order to investigate how the repetition frequency changes under different bias conditions, and more importantly, at high temperatures, the RF spectra were systematically recorded as a function of I_g at 20 and 40 °C, as shown in Fig. 5(a). The repetition frequency at 60 °C is not shown since the laser only exhibited stable mode locking within a small bias condition range at such a
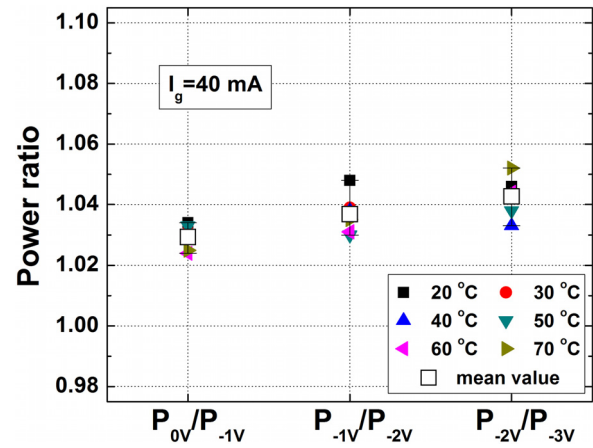
high temperature, which is not suitable for comparison. To simplify the analysis, V_a was fixed at -1.2 V. At each temperature, the frequency decreases consistently and linearly with I_g at the rates of 1.82 and 0.87 MHz/mA for 20 and 40 °C, respectively. This decrease is commonly observed in two-section mode-locked lasers[11,15] and is due to several reasons, all of which originate from the current induced gain section active region temperature increase: increased laser cavity length (L) due to thermal expansion; increased refractive index (n_{eff}) due to gain section bandgap shrinkage.

On the other hand, the frequencies at 40 °C are higher throughout the current range. We interpret it by the decrease in n_{eff} of the laser waveguide caused by the wavelength redshift at higher temperatures as shown in Fig. 5(b). As can be seen from the figure, at a fixed temperature, the lasing wavelength remains almost unchanged with I_g. This indicates that although the gain section active region temperature rises as I_g increases, this rise is actually not so significant. At the same time, the absorber temperature remains unchanged. In contrast, when the
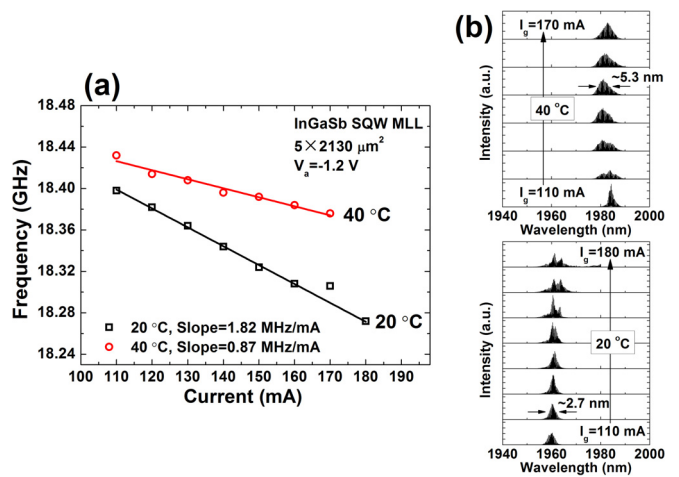

FIG. 5. (a) Repetition frequencies of the laser as a function of I_g when V_a is fixed at -1.2 V at 20 and 40 °C. (b) Optical spectra under the corresponding bias conditions.
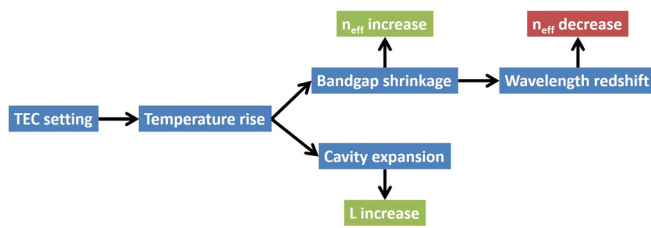
FIG. 6. Frequency tuning mechanism caused by working temperature rise (L: cavity length; n_{eff}: effective refractive index of the laser waveguide). Green blocks show the factors to reduce the repetition frequency, while the red block is the factor that increases the frequency.

working temperature is increased from 20 to 40 °C, it shows a 20 nm jump in the lasing wavelength (from ∼1960 to ∼1980 nm). This jump is a combined effect of the bandgap shrinkages of both the gain section and the absorber section (subsequently changes its absorption peak). It directly results in the n_{eff} decrease and thus leads to a higher repetition frequency. Of course, the above-mentioned temperature related factors which cause the repetition frequency to drop also exist. So when temperature rises, two opposite mechanisms exist simultaneously to affect the repetition frequency, as summarized in Fig. 6. In the case shown in Fig. 5, the wavelength jump related n_{eff} change prevails.

According to the above analysis, several parameters (I_g, V_a, and T) can be adjusted for realizing the repetition frequency tuning or stabilization (with some feedback mechanisms) of a monolithic mode-locked laser to meet the application-required frequencies. This is even more desirable with the consideration of a typical 1% cleaving uncertainty.[24] Taking some practical applications for example, some specific and stable frequencies are required when the mode-locked lasers are used for optical time division multiplexing (OTDM) and clock signal generation,[25] and when the lasers are used to generate frequency combs for dual-comb spectroscopy,[26,27] frequency tuning becomes important.

Moreover, the spectra at 40 °C are generally and markedly wider than those at 20 °C. Taking two symmetric spectra at these two temperatures for example, FWHM of the spectra almost doubles from 2.7 nm at 20 °C to 5.3 nm at 40 °C. It indicates that when the laser is working in the mode locking regime, more longitudinal modes will be locked in phase at 40 °C. A possible reason for this increase is the gain bandwidth increase at high temperatures, similar to what we observed at large negative V_a in our previous modal gain study.[16] This also shows the potential to obtain shorter pulses, and more channels/comb lines can be expected when the laser is used as a multiwavelength light source.

In conclusion, a monolithic two-section InGaSb/AlGaAsSb SQW MLL emitting at 2 μm is demonstrated. The laser is able to lase in the cw mode up to 80 °C, and passive mode locking operation is observed up to 60 °C. It has a T_0 of ∼88 K near room temperature, which is only slightly affected by the absorber bias voltage. This is confirmed by the temperature-independent power ratios before lasing threshold. In the bias range in this work, the repetition frequency increases as a whole by more than 30 MHz when the temperature is raised from 20 to 40 °C, and frequency tuning of ∼130 and ∼60 MHz at 20 and 40 °C was achieved, respectively. The increase as temperature rises could be attributed to the wavelength redshift caused by the absorption peak shift at high temperatures. The spectra at 40 °C are generally and

markedly wider than those at 20 °C. These findings provide guidelines for GaSb-based MLLs to better meet the application-required repetition frequencies even with the presence of unwanted temperature rising.

REFERENCES

[1]U. Keller, Nature **424**, 831 (2003).

[2]S. Kawanishi, IEEE J. Quantum Electron. **34**, 2064 (1998).

[3]E. Rafailov, M. Cataluna, and W. Sibbett, Nat. Photonics **1**, 395 (2007).

[4]X. Li, H. Wang, Z. Qiao, Y. Zhang, C. Niu, C. Tong, and C. Liu, IEEE J. Sel. Top. Quantum Electron. **22**, 1500507 (2016).

[5]A. Gassenq, N. Hattasan, L. Cerutti, J. B. Rodriguez, E. Tournié, and G. Roelkens, Opt. Express **20**, 11665 (2012).

[6]K. Holc, T. Weig, W. Pletschen, K. Köhler, J. Wagner, and U. T. Schwarz, Proc. SPIE **8625**, 862515 (2013).

[7]X. Huang, A. Stintz, H. Li, L. F. Lester, J. Cheng, and K. J. Malloy, Appl. Phys. Lett. **78**, 2825 (2001).

[8]M. Kuntz, G. Fiol, M. Lämmlin, D. Bimberg, M. G. Thompson, K. T. Tan, C. Marinelli, R. V. Penty, I. H. White, V. M. Ustinov, A. E. Zhukov, Yu. M. Shernyakov, and A. R. Kovsh, Appl. Phys. Lett. **85**, 843 (2004).

[9]M. A. Cataluna, E. U. Rafailov, A. D. McRobbie, W. Sibbett, D. A. Livshits, and A. R. Kovsh, IEEE Photonics Technol. Lett. **18**, 1500 (2006).

[10]E. Sarailou and P. Delfyett, Opt. Lett. **41**, 2990 (2016).

[11]T. Sadeev, D. Arsenijević, D. Franke, J. Kreissl, H. Künzel, and D. Bimberg, Appl. Phys. Lett. **106**, 031114 (2015).

[12]M. J. R. Heck, A. Renault, E. A. J. M. Bente, Y.-S. Oei, M. K. Smit, K. S. E. Eikema, W. Ubachs, S. Anantathanasarn, and R. Nötzel, IEEE J. Sel. Top. Quantum Electron. **15**, 634 (2009).

[13]K. Merghem, R. Rosales, S. Azouigui, A. Akrout, A. Martinez, F. Lelarge, G.-H. Duan, G. Aubin, and A. Ramdane, Appl. Phys. Lett. **95**, 131111 (2009).

[14]E. Sooudi, G. Huyet, J. G. McInerney, F. Lelarge, K. Merghem, R. Rosales, A. Martinez, A. Ramdane, and S. P. Hegarty, IEEE Photonics Technol. Lett. **23**, 1544 (2011).

[15]K. Merghem, R. Teissier, G. Aubin, A. M. Monakhov, A. Ramdane, and A. N. Baranov, Appl. Phys. Lett. **107**, 111109 (2015).

[16]X. Li, H. Wang, Z. Qiao, X. Guo, G. I. Ng, Y. Zhang, Z. Niu, C. Tong, and C. Liu, Appl. Phys. Lett. **111**, 251105 (2017).

[17]T. Feng, L. Shterengas, T. Hosoda, A. Belyanin, and G. Kipshidze, ACS Photonics **5**, 4978 (2018).

[18]A. Schliesser, N. Picqué, and T. W. Hänsch, Nat. Photonics **6**, 440 (2012).

[19]J. Geng and S. Jiang, Opt. Photonics News **25**, 34 (2014).

[20]K. Scholle, S. Lamrini, P. Koopmann, and P. Fuhrberg, in Frontiers in Guided Wave Optics and Optoelectronics, edited by B. Pal (InTech, Rijeka, 2010), Chap. 21.

[21]G. W. Turner, H. K. Choi, and M. J. Manfra, Appl. Phys. Lett. **72**, 876 (1998).

[22]L. Shterengas, G. Belenky, M. V. Kisin, and D. Donetsky, Appl. Phys. Lett. **90**, 011119 (2007).

[23]J. O'Gorman, A. F. J. Levi, T. Tanbun-Ek, and R. A. Logan, Appl. Phys. Lett. **59**, 16 (1991).

[24]M. Kuntz, G. Fiol, M. Laemmlin, C. Meuer, and D. Bimberg, Proc. IEEE **95**, 1767 (2007).

[25]D. Arsenijević, M. Kleinert, M. Spiegelberg, M. Stubenrauch, and D. Bimberg, in 17th International Conference on Transparent Optical Networks (ICTON) (2015), p. Tu.B5.3.

[26]Y. Wang, M. G. Soskind, W. Wang, and G. Wysocki, Appl. Phys. Lett. **104**, 031114 (2014).

[27]G. Villares, A. Hugi, S. Blaser, and J. Faist, Nat. Commun. **5**, 5192 (2014).